eNeuro

Research Article: New Research | Sensory and Motor Systems

Angular tuning properties of low threshold mechanoreceptors in isolated rat whisker hair follicles

https://doi.org/10.1523/ENEURO.0175-22.2022

Cite as: eNeuro 2022; 10.1523/ENEURO.0175-22.2022

Received: 4 May 2022
Revised: 20 September 2022
Accepted: 4 November 2022

Angular tuning properties of low threshold mechanoreceptors in isolated rat whisker hair follicles

Akihiro Yamada[1], Hidemasa Furue[2], Jianguo G Gu[1]

[1]Department of Anesthesiology and Perioperative Medicine, University of Alabama at Birmingham, Birmingham, Alabama 35294

[2]Department of Neurophysiology, Hyogo Medical University, Nishinomiya 663-8501, Japan

Corresponding author email address: jianguogu@.uabmc.edu

Number of pages: 32; Number of figures: 7; Number of words for abstract: 250; for introduction: 779; and for discussion: 1129.

Conflict of interest statement: The authors declare no competing financial interests.

Acknowledgments: This study was supported by NIH grants NS109059, DE018661 and DE023090 to J.G.G.

*Correspondence to:

Jianguo G. Gu, M.B., Ph.D.

Department of Anesthesiology and Perioperative Medicine

School of Medicine

University of Alabama at Birmingham, Birmingham, AL 35294

E-mail: jianguogu@uabmc.edu

Abstract: Angular tuning is preferential sensory response to a directional stimulus and is observed in the whisker tactile system. In whisker hair follicles, there are at least three types of low threshold mechanoreceptors (LTMRs): rapidly adapting (RA), slowly adapting type 1 (SA1), and slowly adapting type 2 (SA2). These LTMRs display angular tuning but their properties remain incompletely studied. Here we used isolated rat whisker hair follicles and pressure-clamped single-fiber recordings to study angular tuning of these LTMRs. Angular tuning was determined with impulses elicited by ramp-and-hold deflection of whisker hair in 24 directions each at 15^{o} for a total of 360^{o}. We show that RA display impulses during ramp-up, both ramp-up and ramp-down, or ramp-down dynamic phases. Both SA1 and SA2 respond to angular stimuli with slowly adapting impulses in most angles. However, SA1 and SA2 show rapidly adapting responses in other angles. All the three types of LTMRs display strong angular tuning, and there is no significant difference in angular tuning index among them. Population wise, the majority of SA1 are tuned in the caudal direction, a large part of SA2 are tuned in the rostral direction, and RA are tuned in multiple directions. In the angles showing strong tuning, the three LTMRs respond to increased stimulation amplitudes with increased impulse numbers in a hyperbola relationship, and the responsiveness based on impulse numbers is SA2 > SA1 > RA. Our findings provide new information on angular tuning properties of LTMRs in whisker hair follicles and help to understand directional encoding.

Keywords: Tactile, whisker hair follicle, directional selectivity, angular tuning, low threshold mechanoreceptors, sensory encoding.

Significance Statement

Angular tuning in the whisker tactile system is essential in life of rodents. Here we studied angular tuning of three types of low threshold mechanoreceptors (LTMRs) in whisker hair follicles: rapidly adapting (RA), slowly adapting type 1 (SA1), and slowly adapting type 2 (SA2). All three types of LTMRs display strong angular tuning in response to whisker hair deflection. Population wise, SA1 are largely tuned to the caudal direction, SA2 are tuned mainly to the rostral direction, and RA are tuned to multiple directions. The three LTMRs respond to increased whisker hair deflection amplitudes with increased impulse numbers, and the responsiveness is SA2 > SA1 > RA. Our findings provide new insights into directional encoding by whisker hair follicle LTMRs.

Introduction

The whisker tactile system, from whisker hair follicles in the periphery to the barrel cortex in the brain, is essential for environmental exploration, tactile discrimination, and social interaction in rodents. The rodent whisker tactile system is an important model system in neuroscience for addressing questions such as how neuronal activity encode sensory stimuli, and how the activity of sensory neurons in turn is “read out” in the brain to give rise to sensory perception and behavioral responses (Adibi, 2019). Rodents can perform tactile discrimination such as differentiating the texture and shape of an object by repetitively sweeping their whisker hairs around the object in forward (protraction) and backward (retraction) directions (Adibi, 2019). Touching an object with whisker hairs generates mechanic force within whisker hair follicles. This leads to activation of low threshold mechanoreceptors (LTMRs) and initiates sensory impulses at the terminals of Aβ-afferent nerves in whisker hair follicles (Leiser & Moxon, 2007). The nerve impulses at Aβ-afferent terminals encode tactile information such as magnitude, velocity, frequency, and direction of tactile stimuli, which are then conveyed to the whisker tactile system in the CNS (Lichtenstein *et al.*, 1990; Minnery *et al.*, 2003; Lee & Simons, 2004; Furuta *et al.*, 2020).

Several morphologically distinct types of LTMRs such as Merkel discs, lanceolate endings, and reticular endings (also known as Ruffini-like endings) have been identified within whisker hair follicles (Halata & Munger, 1980; Takahashi-Iwanaga, 2000; Ebara *et al.*, 2002). Functionally, LTMRs in whisker hair follicles can be classified into rapidly adapting (RA), slowly adapting type1 (SA1), and slowly adapting type 2 (SA2) LTMRs based on their responses to ramp-and-hold deflection of whicker hairs (Gottschaldt *et*

80 *al.*, 1973; Sonekatsu & Gu, 2019). RA LTMRs only fire impulses during the ramp
81 (dynamic) phase of hair deflection and do not fire any impulse during the holding (static)
82 phase of hair deflection (Tonomura *et al.*, 2015; Sonekatsu & Gu, 2019). In contrast,
83 SA1 LTMRs and SA2 LTMRs respond to ramp-and-hold hair deflection in both dynamic
84 and static phase. SA1 LTMRs and SA2 LTMRs fire impulses in an irregular manner and
85 a regular manner, respectively (Wellnitz *et al.*, 2010). It has been suggested that ring
86 sinus Merkel discs, reticular or Ruffini-like endings, and lanceolate endings in whisker
87 hair follicles are functionally SA1, SA2 and RA LTMRs, respectively (Halata & Munger,
88 1980; Ebara *et al.*, 2002; Abraira & Ginty, 2013; Sonekatsu & Gu, 2019; Furuta *et al.*,
89 2020) . Molecular mechanisms underlying tactile transduction at Merkel discs have
90 recently been uncovered with Piezo2 channels being identified as mechanical
91 transducers located on Merkel cells and their associated Aβ-afferent terminals (Ikeda *et*
92 *al.*, 2014; Ranade *et al.*, 2014; Woo *et al.*, 2014).
93 Previous *in vivo* studies in rats and mice have shown that RA LTMRs and SA
94 LTMRs display directional selectivity, or angular tuning (Lichtenstein *et al.*, 1990;
95 Shoykhet *et al.*, 2000; Kwegyir-Afful *et al.*, 2008; Furuta *et al.*, 2020). Angular tuning has
96 been observed in neurons along the whisker tactile pathways including the trigeminal
97 ganglion, brainstem, thalamus, and barrel cortex (Lichtenstein *et al.*, 1990; Minnery *et*
98 *al.*, 2003; Lee & Simons, 2004; Hemelt *et al.*, 2010). Angular tuning is normally defined
99 as responses to directional deflections of principal whisker hairs that evoke the largest
100 response magnitude. Angular tuning is also observed in mouse body hair follicle
101 lanceolate endings which are RA LTMRs derived from Aδ-afferent endings (Rutlin *et al.*,
102 2014). The angular tuning of RA LTMRs in body hair follicles is largely attributable to the

103 directional location of mechanoreceptors within the body hair follicles (Rutlin *et al.*,
104 2014). Directional location of mechanoreceptors within whisker hair follicles also is
105 suggested to attribute to angular tuning of SA1 LTMRs in rat whisker hair follicles
106 (Furuta *et al.*, 2020). However, angular tuning of RA LTMRs in rat whisker hair follicles
107 does not appear to be related to locations of their mechanoreceptors (Furuta *et al.*,
108 2020).

109 Previous studies on angular tuning of LTMRs in whisker hair follicles are
110 performed *in vivo* in anesthetized rats and mice using extracellular recordings made
111 from trigeminal ganglion neurons or intra-axon recordings made from infraorbital nerves
112 (Lichtenstein *et al.*, 1990; Kwegyir-Afful *et al.*, 2008; Furuta *et al.*, 2020). Angular tuning
113 measured *in vivo* is affected by several factors, including intrinsic angular tuning
114 properties of LTMRs within whisker hair follicles as well as tissue mechanics (or
115 stiffness) of the skin that surrounds whisker hair follicles, and the muscle as well as
116 connective tissues that attached to whisker hair follicles (Bush *et al.*, 2016). In addition,
117 anesthesia used in *in vivo* studies may affect impulse activity of LTMRs and thereby
118 affecting the measurement of angular tuning. In the present study, to investigate the
119 intrinsic angular tuning properties of LTMRs without the influence of the tissues
120 surrounding whicker hair follicles, we used isolated whisker hair follicles and pressure-
121 clamped single-fiber recording technique.

122

123 **Material and methods**

124 ***Ex vivo* whisker hair follicle preparations**

Sprague-Dawley rats of both male and female weighing 300 to 500 g were used for making *ex vivo* whisker hair follicle preparations. Animal care and use conformed to NIH guidelines for care and use of experimental animals. Experimental protocols were approved by the Institutional Animal Care and Use Committee (IACUC) at the University of Alabama at Birmingham. In brief, animals were anesthetized with 5% isoflurane and then sacrificed by decapitation. Whisker pads were dissected out from orofacial areas of rats by using a pair of dissecting scissors and placed in a 35-mm petri dish that contained Krebs bath solution (see below). Under a dissection microscope, fat tissues that covered whisker hair follicles were removed by using a pair of fine tweezers to expose individual whisker hair follicles. Whisker hair follicles located at the central region of the whisker pad including B2, B3, C2, C3, D2, D3, and D4 whisker hair follicles together with their whisker afferent bundles and hair shafts were then gently pulled out from both right and left whisker pads. The capsule of each whisker hair follicle was cut open at the end part of the capsule to facilitate solution exchange in the whisker hair follicle. Each whisker hair follicle was affixed on the sylgard-coated bottom of a recording chamber with tissue pins. The end of the whisker afferent bundle was sharply cut with a surgical knife and the nerve bundle was then affixed to the bottom of the recording chamber by a U-shaped tissue anchor. The *ex vivo* whisker hair follicle preparation was submerged in Krebs bath solution contained (in mM): 117 NaCl, 3.5 KCl, 2.5 $CaCl_2$, 1.2 $MgCl_2$, 1.2 NaH_2PO_4, 25 $NaHCO_3$ and 11 glucose. The pH of the Krebs bath solution was adjusted to 7.3 with HCl or NaOH and osmolarity adjusted to 325 mOsm with sucrose. The Krebs solution was saturated with 95% O_2 and 5% CO_2 during experiments.

Pressure-clamped single-fiber recordings from whisker afferent never fibers

The pressure-clamped single-fiber recording was performed to measure impulses in response to whisker hair deflection in the same manner described in our previous studies (Sonekatsu & Gu, 2019; Sonekatsu *et al.*, 2020). In brief, the recording chamber was mounted on the stage of an Olympus BX50WI microscope. The whisker hair follicle preparation was briefly exposed to a mixture of 0.1% dispase II plus 0.1% collagenase in the Krebs bath solution for 1 min, and the enzymes were then quickly washed off with the normal Krebs bath solution. This gentle enzyme treatment was to help separating individual afferent fibers so that a single fiber could be aspirated into the recording electrode and pressure-clamped for single fiber recordings. Recording electrodes for pressure-clamped single-fiber recordings were made by thin-walled borosilicate glass tubing without filament (inner diameter 1.12 mm, outer diameter 1.5 mm, World Precision Instruments, Sarasota, FL). They were fabricated by using P-97 Flaming/Brown Micropipette Puller (Sutter Instrument Co., Novato, CA) and the tip of each electrode was fire polished by a microforge (MF-900, Narishige) and final tip size was 10 to 12 μm in diameter. The recording electrode was filled with Krebs bath solution, mounted onto an electrode holder which was connected to a high-speed pressure-clamp (HSPC) device (ALA Scientific Instruments, Farmingdale, NY) for fine controls of intra-electrode pressures. Under a 40x objective, the end of a single whisker afferent nerve was first separated from whisker afferent nerve bundle by applying a low positive pressure (~10 mmHg or 0.19 Psi) from the recording electrode. The end of the single nerve fiber was then aspirated into the recording electrode by a negative pressure at

171 approximately -10 mmHg. Once the end of the nerve fiber entered into the recording
172 electrode in approximately 10 μm, the electrode pressure was readjusted to -3 ± 2
173 mmHg and maintained at the same pressure throughout the experiment. Nerve
174 impulses evoked by whisker hair deflection (see below) and conducted along a single
175 whisker afferent fiber were recorded under the I_0 configuration and amplified using a
176 Multiclamp 700B amplifier (Molecular Devices, Sunnyvale, CA). Electrical signals were
177 amplified 100 to 1000 times and sampled at 25 kHz with AC filter at 0.1 Hz and Bessel
178 filter at 3 kHz under AC membrane mode (Digidata 1440A, Molecular Devices). All
179 experiments were performed at the room temperature of 23°C to 24°C.
180
181 **Angular stimulation of whisker hairs**
182 Whisker hair was trimmed to have the length of approximately 8 mm. A
183 mechanical probe, made with an L-shaped glass pipette, was mounted on a pipette
184 holder and controlled by a programmable manipulator (MPC-325, Sutter). The trimmed
185 hair shaft was fit into the end of the mechanical probe, and the position of the whisker
186 hair shaft was adjusted to neutral position at which the hair shaft was not bended
187 toward any direction. To produce angular deflection of the whisker hair, the mechanical
188 probe was moved in a ramp-and-hold manner in 24 directions at the increment of 15°
189 each direction (360° total). The interval between any two angular deflections was 5
190 seconds. Unless otherwise specified, the ramp-and-hold deflection consisted of a 234
191 ms ramp-up to 200 μm (dynamic phase), 4.75 s hold at 200 μm (static phase), and a
192 234 ms ramp-down to the original position. All angular deflections were made by a
193 programmable manipulator that was controlled by a software (Multi-Link™, Sutter), and

194 the probe movement as well as nerve impulses were simultaneously recorded using the
195 pClamp 10 software.

196 In the present study, whisker hair follicles at the central region of both right and
197 left whisker pads were used. The angular deflection used the afferent root of each
198 whisker hair follicle as a reference point, which is approximately 45^{o} in dorsal-caudal
199 direction in the head axes *in vivo as was determined anatomically*. Angular deflection of
200 each whisker hair in our recording chamber started first in the direction same as its
201 afferent root's direction, i.e. 45^{o} in dorsal-caudal direction in the coordinate of head axes.
202 In each experiment, disregard using a left or a right whisker hair follicle, the angular
203 deflection was applied clockwise in 15^{o} increment. The conversion from the afferent-
204 root-referenced coordinate to the *in vivo* head axes was as follow. For a left-side
205 whisker hair follicle, 45^{o}, 135^{o}, 225^{o} and 315^{o} clockwise whisker hair deflections in
206 reference to the afferent root were equivalent to *in vivo* whisker hair deflection in caudal,
207 ventral, rostral and dorsal, directions, respectively. For a right-side whisker hair follicle,
208 45^{o}, 135^{o}, 225^{o} and 315^{o} clockwise whisker hair deflections in reference to the afferent
209 root were equivalent to *in vivo* whisker hair deflection in dorsal, rostral, ventral, and
210 caudal directions, respectively. All other angles could be converted to the head axes in
211 the same manner.

212

213 **Data analysis**

214 Data were collected from whisker hair follicles of 3 male and 22 female animals.
215 We observed no signs that there were differences between the male and female rats,
216 thus their data were considered together for data analysis. Impulses recorded from

single whisker afferent fibers were analyzed using the Clampfit 10 software. Unless otherwise specified, impulses induced during the dynamic phase (234 ms) and static phase (4.75 s) of angular whisker hair deflection were combined together to represent angular response. Impulse numbers or frequency were used to represent angular response of LTMRs to whisker hair deflection. SA1 and SA2 LTMRs were defined by the coefficient of variance (CV) of inter-impulse intervals, with CV value ≥ 0.5 being considered as SA1 LTMRs and CV < 0.5 as SA2 LTMRs, based on previous studies on the regularity of SA LTMRs in mouse hair skin (Wellnitz *et al.*, 2010) and whisker hair follicles (Sonekatsu & Gu, 2019). In the cases when CV values were at the borderline of 0.5, we also used impulse frequency to aid for classifying SA1 (lower frequency) or SA2 (higher frequency) (Sonekatsu & Gu, 2019). Sensitive angles were defined as the angles at which the angular responses (impulse numbers) were ≥ 80% of maximum angular response. Tuning direction was the vector of angular response. Four general tuning directions were defined, caudal (rostral-to-caudal ± 45^{o}), ventral (dorsal-to-ventral ± 45^{o}), rostral (caudal-to-rostral ± 45^{o}), and dorsal (ventral-to-dorsal ± 45^{o}) direction. The angle size of high-sensitivity was defined as the size of the angle at which responses were ≥ 80% of maximal impulses. Tuning index was calculated and used as a measure of how strong angular tuning was for individual LTMRs (Taylor & Vaney, 2002). The tuning index (D) was calculated as D = Σvi /Σri (i.e., D = vector sum/scalar sum), where vi are vector magnitudes pointing in the direction of the stimulus and having length, ri, equal to the number of impulses recorded during that stimulus (Bellavance *et al.*, 2010). D can range from 0, when the responses are equal in all stimulus directions, to 1, when a response is obtained only for a single stimulus

direction (Bellavance *et al.*, 2010). Curve fitting for the relationship between whisker hair deflection amplitude and LTMR response were made with a hyperbola equation Y = (Ymax*X)/(Kd+X), where Y is the response (impulse numbers), X is whisker hair deflection amplitude, and Kd is deflection amplitude at which 50% of maximal response is produced. All data analyses were performed using Graph Pad Prism (version 8). Unless otherwise indicated, all data were reported as mean ± SEM of *n* independent observations. Statistical significance was evaluated using the Kruskal-Wallis (nonparametric) test with Dunn's post hoc tests for multiple group comparison, Mann-Whitney (nonparametric) test or Student's t tests for two group comparison. Differences were considered to be significant with *p < 0.05, **p < 0.01, ***p < 0.001, and not significant (ns) with p ≥ 0.05.

Results

Angular response of rapidly adapting (RA) LTMRs

We used *ex vivo* rat whisker hair follicle preparation and applied pressure-clamped single-fiber recording technique to study responses of LTMRs to angular deflection of rat whisker hairs (Figure 1A1-3). In each recording, the afferent root of each whisker hair follicle was used as a reference point so that angular deflection of a whisker hair in our recording chamber can be converted to the deflection directions in head axes *in vivo* (Figure 1A1-3). As shown in Figure 1A1-A3, for whisker hair follicles at the central region of whisker pads, afferent root of these whisker hair follicles tilted approximately 45^{o} toward dorsal-caudal direction (Figure 1A2-3). In experiments, for either a left side or a right side hair follicle, the first hair deflection was applied in the

same direction as its afferent root's direction, i.e. 45° dorsal-caudal direction. Subsequent whisker hair deflections were applied clockwise in a 15° increment (Figure 1A2-3). Angular responses were measured as whisker afferent impulses in response to ramp-and-hold deflection of a whisker hair in 24 different directions for a total of 360° (Figure 1B).

In one type of LTMR response, angular deflection in each direction evoked impulses only during the dynamic phase. Using an angular whisker hair deflection of 200 μm, impulses could be elicited in many angles and phases, including during ramp-up, both ramp-up and ramp-down, or ramp-down (Figure 1B). In some angles, deflection of whisker hairs failed to elicit any impulse (null angle). Regardless of direction, no impulse was elicited during the static phase of the ramp-and-hold whisker hair deflection. Thus, these were RA LTMRs. The average sizes of angles for which RA LTMRs responded only in ramp-up phase were 111 ± 12° (n = 21), in both ramp-up and ramp-down phases were 100 ± 15° (n = 21), and only in ramp-down dynamic phase was 99 ± 13° (n = 21, Figure 1C), with no significant difference observed. The sizes of the angles showing no response or null angle was 50 ± 12° (n = 21, Figure 1C), and was significantly narrower than those with responses ($p < 0.05$). Average maximal RA impulse frequency was 54.9 ± 5.2 Hz (n = 21, Figure 1D) for the angular responses occurring during ramp-up phase, significantly higher than that during ramp-down phase (39.5 ± 5.6 Hz, n = 21, $p < 0.001$, Figure 1D). Average maximal impulse count was 12.9 ± 1.2 (n = 21, Figure 1E) for the angular responses occurring during ramp-up phase, significantly more than that during ramp-down phase (9.2 ± 1.3, n = 21, $p < 0.001$, Figure 1E).

To quantitatively determine tuning properties of RA LTMRs, impulses evoked by 200 µm whisker hair deflection at each angle were plotted in the polar coordinate system (polar plot), and tuning direction was then calculated as a vector of the overall impulses (Figure 2A, B). The data were grouped into four general angular categories (Figure 2A), caudal direction (caudal ± 45^{o}), dorsal direction (dorsal ± 45^{o}), rostral direction (rostral ± 45^{o}), and ventral direction (ventral ± 45^{o}). RA LTMRs showed strong angular tuning, and the ramp-up and ramp-down responses usually were tuned in opposite directions (Fig. 2A). More RA LTMRs showed dorsal and ventral angular tuning in the ramp-up phase, and caudal and rostral angular tuning in the ramp-down phase (Figure 2B). However, population wise, RA LTMRs were tuned to multiple directions rather than to a dominant direction (Figure 2B). The angle sizes of high sensitivity, defined as the sizes of angles at which impulse count was ≥ 80% maximal angular response, ranged from angle sizes of 15 to 150^{o} for RA LTMRs, and most had narrow angles with the sizes from 15 to 60^{o} (Figure 2C). Overall, the angle sizes of high sensitivity for RA LTMRs were 36 ± 7^{o} (n = 21). Tuning index has been commonly used to describe how strong angular tuning is in response to angular stimulation, with the tuning index value of 0 being no angular tuning and 1 being the strongest tuning. Tuning index was determined for each RA LTMR in response to angular stimulation. For ramp-up responses, the tuning index was in the range of 0.2 to 1 in all 21 recordings, but the majority of recordings had a tuning index of 0.6 to 0.8 (Figure 2D). For ramp-down responses, the tuning index was also in the range of 0.2 to 1 in all 21 recordings but the majority of recordings had a tuning index of 0.8 to 0.9 (Figure 2D). Overall, the tuning index was 0.626 ± 0.041 (n = 21) for ramp-up responses and 0.640 ± 0.045 (n = 21) for

309 ramp-down responses (Figure 2D). These results indicate that individual RA LTMRs
310 mostly had strong angular tuning.

311 At the most sensitive tuning direction where maximal angular response was
312 elicited, we quantitatively measured the relationship between whisker hair deflection
313 amplitudes and RA LTMR responses in rat whisker hair follicles (Figure 2E&F). We
314 tested whisker hair deflections ranging from 10 μm to 500 μm. RA impulses showed
315 progressive increases in response to whisker hair deflections from 10 to 300 μm, and
316 the response appeared to be plateaued subsequently. The deflection amplitude-
317 response relationship could be fit with a hyperbola equation Y = (Ymax*X)/(Kd+X),
318 where Y is response (impulse numbers), X is deflection amplitude, and Kd is deflection
319 amplitude at which 50% of maximal response is produced (Figure 2F). Overall, Kd value
320 was 25 ± 11 μm (n = 3 - 5, Figure 2F) for the hyperbola relationship between whisker
321 hair deflection amplitude and RA LTMR response.
322
323 **Angular response of slowly adapting type 1 (SA1) LTMRs**
324 In the second type of LTMR responses, an angular deflection of 200 μm evoked
325 impulses during both the dynamic and static phase for many angles (Figure 3A). The
326 impulses displayed high irregularity in inter-impulse intervals (see Figure 3E&F) and
327 thereby were SA1 responses (Wellnitz *et al.*, 2010). However, for other angles the
328 whisker hair deflection evoked impulses only during the dynamic phases of ramp-up,
329 ramp-up and ramp-down (up & down), or ramp-down (Figure 3A&B), and collectively we
330 termed these impulses RA-like responses. In addition, in some angles impulses
331 occurred during and after ramp-down phase (Figure 3B), which were termed post-ramp

responses in the present study. There were also angles at which whisker hair deflections failed to elicit any impulses (null angle, Figure 3A). For all SA1 LTMRs tested with whisker hair deflection, the sizes of angles that elicited impulses in both the dynamic and static phase (SA1 angle) were 198 ± 16^{o} (n = 19), which were significantly greater than the sizes of angles that elicited impulses only in the dynamic phase (RA-like angle, 73 ± 14^{o}, n = 19, $p < 0.001$, Figure 3C). SA1 angle sizes were also significantly larger than that the sizes of the post-ramp impulse angles (52 ± 18^{o}, n = 19, $p < 0.001$, Figure 3C) and the null angles (27 ± 9^{o}, n = 19, $p < 0.001$, Figure 3C). For RA-like responses, the sizes of angles that elicited impulses in ramp-up only, ramp-up and ramp-down, and ramp-down only were 13 ± 5^{o} (n = 19), 25 ± 9^{o} (n = 19), and 35 ± 12^{o} (n = 19), respectively, and no significant difference was observed (Figure 3D).

At the most sensitive angles where impulses occurred in both the dynamic and static phase of whisker hair deflection, the instantaneous frequency calculated from inter-impulse intervals was highly irregular (Figure 3E). The coefficient of variance of inter-impulse intervals was 1.11 ± 0.19 (n = 19 recordings, Figure 3F), indicating high irregularity of inter-impulse intervals. The result of irregular impulses indicated these were SA1 LTMRs. For whisker hair deflection of 200 μm in the most sensitive angle, impulse frequency was 69.3 ± 8.0 Hz (n = 19) in the dynamic phase, significantly higher than that in the static phase (15.6 ± 2.8 Hz, n = 19, $p < 0.001$, Figure 3G).

To quantitatively determine tuning properties of SA1 LTMRs, impulses evoked by 200 μm whisker hair deflection at each angle were plotted in the polar coordinate system, and tuning direction was then calculated as a vector of the overall impulses (Figure 4A, B). Of a total 19 SA1 LTMRs recorded, 11/19 (57.9%) were tuned to the

355 caudal direction, 4/19 (21.1%) to the dorsal direction, 3/19 (15.8%) to the ventral
356 direction, and 1/19 (5.3%) to the rostral direction (Figure 4B). Thus, the caudal direction
357 was the most common tuning direction for SA1 LTMRs in rat whisker hair follicles
358 (Figure 4A&B). We determined the angle sizes of high sensitivity for each SA1 LTMR
359 recorded. Of 19 SA1 LTMRs recorded, 17/19 (89.5%) had the angle sizes of high
360 sensitivity between 30 to 90^{o} (Figure 4C). Overall, the average angle size of high
361 sensitivity of these SA1 LTMRs was 52.1 ± 4.5^{o} (Figure 4C, n = 19). Tuning index was
362 determined for SA1 LTMRs. Tuning index ranged from 0.4 to 1 in all 19 recordings, but
363 a large fraction of recordings (8/19) had tuning index from 0.7 to 0.8 (Figure 4D),
364 suggesting many SA1 LTMRs were highly tuned angularly. Overall, tuning index was
365 0.68 ± 0.03 (n = 19, Figure 4D), indicating a strong angular tuning of SA1 LTMRs in rat
366 whisker hair follicles.

367 Having determined the angular tuning, we further quantitatively measured, at the
368 most sensitive tuning direction, the relationship between whisker hair deflection
369 amplitude and response of SA1 LTMRs. The deflection amplitudes from 10 μm to 500
370 μm were tested. SA1 impulses showed a progressive increase in impulse numbers with
371 increased deflection amplitudes up to 300 μm and nearly reached to a plateau level
372 afterward (Figure 4E&F, n = 4). The deflection amplitude-response relationship could be
373 best fit into the hyperbola equation with a Kd value of 105 ± 34 μm (n = 4).

374

375 **Angular response of slowly adapting type 2 (SA2) LTMRs**

376 In the third type of LTMR response, 200 μm angular deflection of whisker hairs
377 evoked impulses during both the dynamic and static phases for many angles (Figure

5A). The impulses displayed high regularity in inter-impulse intervals (see Figure 5E&F) and thereby were SA2 responses (Wellnitz *et al.*, 2010). However, for some angles whisker hair deflection evoked impulses only during the ramp-up, ramp-up and ramp-down (up & down), or ramp-down dynamic phase (RA-like, Figure 5A&B). In addition, in some angles, impulses occurred during and after ramp-down phase (post-ramp, Figure 5B). There were also angles at which whisker hair deflections failed to elicit any impulses (null angle, Figure 5A). For all SA2 LTMRs tested with whisker hair deflection, the sizes of angles that elicited impulses in both the dynamic and static phases (SA2 angle) were 200 ± 13^{o} (n = 23), which was significantly greater than the sizes of RA-like angles that elicited impulses in dynamic phase only (46 ± 9^{o}, n = 23, $p < 0.001$, Figure 5C). The sizes of SA2 angles were also significantly larger than the sizes of angles of the post-ramp impulses (31 ± 10^{o}, n = 23, $p < 0.001$) and the null angles (78 ± 16^{o}, n = 23, $p < 0.001$, Figure 5C). For RA-like responses, the sizes of the angles that elicited impulses in ramp-up only, ramp-up and ramp-down, and ramp-down only were 19 ± 6^{o} (n = 23), 7 ± 2^{o} (n = 23), and 20 ± 6^{o} (n = 23), respectively, and no significant difference was observed (Figure 5D).

At the highest sensitive angles, the instantaneous frequency calculated from the inter-impulse intervals showed high regularity (Figure 5E). The coefficient of variance of inter-event interval of impulses elicited at the highest sensitive angles was 0.32 ± 0.02 (n = 23), indicating high regularity of the impulses (Figure 5F). The result of highly regular impulses indicated these were SA2 LTMRs. For whisker hair deflection of 200 μm at the most sensitive angles, impulse frequency was 84.2 ± 8.8 Hz (n = 23) in the

400 dynamic phase, significantly higher than that in the static phase (33.2 ± 4.6 Hz, n = 23,
401 $p < 0.001$, Figure 5G).

402 We determined tuning direction of SA2 LTMRs using the polar plot for the
403 impulses evoked by 200 μm whisker hair deflection (Figure 6A&B). Of a total 23 SA2
404 LTMRs recorded, 11/23 (47.8%) SA2 were tuned to the rostral direction, 7/23 (30.4%) to
405 the ventral direction, 4/23 (17.4%) to the caudal direction, and 1/23 (4.3%) to the dorsal
406 direction (Figure 6B). Thus, the rostral direction was the most common and dorsal
407 direction the least common tuning direction for SA2 LTMRs in rat whisker hair follicles
408 (Figure 6A&B).

409 We determined the angle sizes of high sensitivity of SA2 LTMRs recorded from
410 whisker afferent fibers. Of 23 SA2 LTMRs recorded, the angle of high sensitivity was in
411 the size range from 30 to 150^{o}, and more than 50% SA2 LTMRs recorded showed the
412 angle size of high sensitivity in 30 to 60^{o} (Figure 6C). Overall, the average angle size of
413 high sensitivity of these SA2 LTMRs were 60.0 ± 5.9^{o} (n = 23, Figure 6C). Tuning index
414 was determined for each SA2 LTMR recorded with angular stimulation. Tuning index
415 was in the range of 0.3 to 1 in all 23 recordings, and the majority of recordings had
416 tuning index of 0.7 to 0.8 (Figure 6D). Overall, tuning index was 0.659 ± 0.035 (n = 23,
417 Figure 6D), indicating a strong angular tuning in SA2 LTMRs in rat whisker hair follicles.
418 At the most sensitive tuning direction, we quantitatively measured the relationship
419 between whisker hair deflection amplitude and SA2 response in rat whisker hair follicles
420 (Figure 6E&F, n = 6). We tested deflection amplitudes ranging from 10 μm to 500 μm.
421 SA2 impulses showed a progressive increase in a manner that could be described by
422 the hyperbola equation with a Kd value of 167 ± 48 μm (n = 6, Figure 6F).

Comparison of angular tuning of SA1, SA2 and RA LTMRs in whisker hair follicles

Figure 7 compares and contrasts the angular sensitivities of the three different LTMR types already shown in Figures 1-6. Data were the responses of these LTMRs to angular deflection of whisker hairs at the amplitude of 200 μm. All three types of LTMRs showed strong angular tuning with high tuning index, and tuning indexes were not significantly different among the three types of LTMRs (Figure 7A). While SA1 and SA2 LTMRs showed similar average angle sizes of high sensitivity, RA displayed significantly narrower angles of high sensitivity in comparison with the angles of high sensitivity of both SA1 ($p < 0.001$, Figure 7B) and SA2 LTMRs ($p < 0.01$, Figure 7B). The angle sizes of null response, for which the angular stimulation did not evoke any impulses, were significantly narrower in SA1 LTMRs than that of SA2 LTMRs ($p < 0.05$, Fig. 7C). Determined at the most sensitive angles, the impulse frequency in dynamic phase was significantly lower in RA LTMRs ($n = 21$, $p < 0.05$) than in SA2 LTMRs ($n = 23$, Figure 7D); the impulse frequency in the dynamic phase was not significantly different between SA1 LTMRs ($n = 19$), and SA2 LTMRs ($n = 23$, Figure 7D). For the static phase, the impulse frequency of SA2 LTMRs ($n = 23$) was nearly significantly higher than that of SA1 LTMRs ($n = 19$, $p < 0.06$, Fig. 7E); RA LTMRs did not respond to angular whisker hair deflection ($n = 21$, Figure 7E).

Discussion

Using acutely isolated whisker hair follicles of rats and pressure-clamped single-fiber recording technique, the present study investigated responses of RA, SA1, and

446 SA2 LTMRs in whisker hair follicles to directional stimuli to explore how these LTMRs
447 encode directional tactile information. We show that all three LTMRs have strong
448 angular tuning. Population wise, a large portion of SA1 LTMRs and SA2 LTMRs are
449 tuned in the caudal-to-rostral and the rostral-to-caudal directions, respectively, and RA
450 LTMRs are tuned to multiple directions without a dominant one. In the most sensitive
451 direction, all three LTMRs encode amplitude of whisker hair deflection, and the
452 responsiveness based on impulse numbers is SA2 > SA1 > RA. The present study
453 provides new information on angular tuning of the three types of LTMRs in whisker hair
454 follicles of rats.

455 There are several technical differences between the present work and several
456 previous studies. First, the present study used isolated whisker hair follicles and
457 performed *in vitro* recordings while previous studies performed *in vivo* recordings in
458 anesthetized animals (Lichtenstein *et al.*, 1990; Kwegyir-Afful *et al.*, 2008; Furuta *et al.*,
459 2020). The use of isolated whisker hair follicles allows us to study tuning properties of
460 LTMRs within whisker hair follicles without potential complications due to mechanics of
461 tissues that surround whisker hair follicles (Bush *et al.*, 2016). Second, in the present
462 study we tested 24 angular directions to map angular response at each direction. On
463 the other hand, previous studies tested 4 or 8 directions (Lichtenstein *et al.*, 1990;
464 Kwegyir-Afful *et al.*, 2008; Rutlin *et al.*, 2014; Furuta *et al.*, 2020). Our study with 24
465 angular directions allowed us to observe transitional changes in angular responses. For
466 example, we show that, both SA1 and SA2 LTMRs display rapidly adapting responses
467 in some stimulation angles. For RA LTMRs, we also observed transitional changes,
468 from ramp-up response only, both ramp-up and ramp-down response, to ramp-down

response only. To our knowledge, these transitional changes have not been characterized previously. We have observed impulses after the end of ramp-down phase (post-stimulation responses) in some SA1 and SA2 LTMRs, which may be because the mechanical tension of these LTMRs did not return to the basal level immediately after the withdraw of the mechanical probe. The third difference between the present study and previous studies is that we performed recordings from nerve fibers that innervate individual whiskers being studied while previous recordings were performed in a blinded manner from trigeminal neurons (Lichtenstein *et al.*, 1990; Kwegyir-Afful *et al.*, 2008). In addition to the above differences, the deflection ramp speed and amplitude as well as holding period were also different between the present work and previous studies. For example, our ramp-and-hold stimulation is relatively slower in speed, smaller in amplitude, and longer in holding period in comparison with previous studies (Lichtenstein *et al.*, 1990; Shoykhet *et al.*, 2000).

Individually, each RA, SA1, or SA2 LTMR has strong angular tuning as shown in the present study. Based on calculated tuning index, angular tuning of these three types of LTMRs are equally well, and there is no significant difference in tuning index among the three types of LTMRs. However, we found that RA LTMRs had relatively narrower angles of high sensitivity in comparison with the angle sizes of SA1 and SA2 LTMRs, suggesting that RA LTMRs may be better angularly tuned than SA1 and SA2 LTMRs. SA2 had relatively broader null response angles in comparison with SA1 LTMRs, suggesting that SA2 may be better angularly tuned than SA1 LTMRs. In contrast, angular tuning was shown to be better in SA LTMRs than RA LTMRs in previous *in vivo* studies with recordings from TG neurons in anesthetized rats and mice showed better

(Lichtenstein *et al.*, 1990; Kwegyir-Afful *et al.*, 2008). The discrepancy in the degree of angular tuning between SA and RA LTMRs may be due to the sub-classification of SA LTMRs into SA1 LTMRs and SA2 LTMRs in the present study. We show that at the best tuning angle for each LTMR, response to whisker hair deflection increases with the increases of whisker hair deflection amplitudes. The responsiveness based on impulse numbers is SA2 > SA1 > RA. Our results are consistent with a previous study showing that SA encode stimulation amplitude better than that of RA LTMRs (Shoykhet *et al.*, 2000).

We show, as a whole population, SA1 LTMRs are tuned in the rostral-to-caudal direction since a large portion of SA1 LTMRs have response vectors pointing to the caudal direction. In contrast, a relatively large portion of SA2 LTMRs are tuned in the caudal-to-rostral direction. Our results contradict previous *in vivo* studies which showed that individual SA LTMRs were tuned to different directions rather than preferentially to a certain direction (Lichtenstein *et al.*, 1990; Kwegyir-Afful *et al.*, 2008). It should be noted that the previous *in vivo* recordings did not sub-classify SA LTMRs into SA1 and SA2 LTMRs (Lichtenstein *et al.*, 1990; Shoykhet *et al.*, 2000; Kwegyir-Afful *et al.*, 2008), which may be a reason of having weaker angular tuning in previous studies. In a more recent *in vivo* study, strong angular tuning was also shown in individual SA1 LTMRs being recorded but the small number of recordings in that study could not allow for determining population wise if SA1 LTMRs have angular tuning to a certain direction (Furuta *et al.*, 2020). Population wise, the lack of angular tuning for SA LTMRs in previous studies may be due to the opposite tuning directions of SA1 LTMRs and SA2 LTMRs since the previous studies did not sub-classify SA into SA1 and SA2

(Lichtenstein *et al.*, 1990; Kwegyir-Afful *et al.*, 2008). In contrast to SA1 and SA2 LTMRs, RA LTMRs as a population display much weaker angular tuning in comparison with SA1 and SA2 LTMRs. This is evidenced by our finding that overall RA LTMRs are not overwhelmingly outnumbered in a given direction although individual RA LTMRs show strong angular tuning. The lack of strong angular tuning for RA LTMRs as a whole population is in sharp contrast with RA LTMRs in body hair follicles of mice which were shown to be tuned in the rostral-to-caudal direction (Rutlin *et al.*, 2014).

The angular tuning of the LTMRs in whisker hair follicles raises a question as whether there are tactile blind spots in whisker tactile system. Tactile information and resulting behavioral response are most likely the results of population responses of LTMRs to tactile stimuli. Since RA LTMRs in whisker hair follicles as a whole population respond almost equally well to whisker deflection in every direction, there should be no tactile blind spot in rats in terms of using their RA LTMRs of whisker hair follicles to detect stimuli from different directions. Mechanisms underlying angular tuning of LTMRs in whisker hair follicles are not fully understood. It has been thought that uneven distribution of the terminals of LTMRs within whisker hair follicles may contribute to angular tuning of LTMRs (Furuta *et al.*, 2020). Consistently, the caudal-to-rostral angular tuning of Aδ-afferent RA LTMRs in body hair follicles is attributed to directional expression of mechanoreceptors (Abraira & Ginty, 2013). More recently, it has also been shown that the angular tuning of SA1 LTMRs in whisker hair follicles is attributed to the directional location of SA1 afferent terminals in whisker hair follicles (Furuta *et al.*, 2020). In addition to the location of mechanoreceptors, angular tuning in terms of the degree of sensitive and null angles may be partially attributed to the areas of LTMR

terminal arborization. Furthermore, the viscoelastic properties of tissues that surround LTMR terminals may also contribute to the degree of sensitive and null angles (Bush *et al.*, 2016). The viscoelastic properties of these tissues may also play a role in the transitional responses observed in all three types of LTMRs. The use of isolated whisker hair follicles and pressure-clamped single-fiber recordings as shown in the present study may provide a useful model to further study the underlying mechanisms of angular tuning of LTMRs within whisker hair follicles and to help understand neuronal encoding of directional tactile information.

548 **Figure legends**

549 **Figure 1. Angular responses of RA LTMRs in whisker hair follicles of rats**

550 **A1-A3)** Positions of a left and a right whisker hair (orange), their follicles (red) and
551 afferent roots (blue) in head axes viewed from top of the head (A1), left side (A2 top)
552 and right side (A3 top). In the diagrams, only one hair follicle with its afferent root on
553 each side is shown for clarity. For either the left (A2 top panel) or the right (A3 top panel)
554 whisker hair follicle, its afferent root tilts approximately 45^{o} toward dorsal-caudal
555 direction. The positions described here are applicable for the whisker hair follicles
556 located at the central region of whisker pads. A2 bottom panel and A3 bottom panel
557 illustrate *in vitro* recording of afferent impulses while whisker hair is angularly deflected.
558 In experiments, for either a left side or a right side hair follicle, the first hair deflection
559 was always applied in the same direction as its afferent root's direction (solid black
560 arrow indicated, 45^{o} dorsal-caudal direction). Whisker hair deflections were
561 subsequently applied clockwise in a 15^{o} increment. **B**) Sample trace (top panel) shows
562 RA LTMR impulses in response to ramp-and-hold whisker hair deflection in 24 angular
563 directions each at the amplitude of 200 μm. The recording was from a left C2 whisker
564 hair follicle. The scale bar to the right indicates the angle size of whisker hair deflection.
565 The 24 directions of whisker hair deflection started with 1st deflection in afferent root
566 direction. Bottom three traces are impulses at the expanded time scale from arrow-
567 indicated angles in the top panel, one angle induced responses only in the ramp-up
568 phase (left), another angle induced impulses in both the ramp-up and ramp-down
569 phases (middle), and the third angle induced impulses only in the ramp-down phase
570 (right). In all 24 directions, no impulses were evoked during the static phase. **C**)

571 Summary data (n = 21) of the sizes of the angles showing impulses only in the ramp-up
572 phase, impulses in both the ramp-up and ramp-down phases, impulses only in the
573 ramp-down phase, and the sizes of angles showing no response (null angle). **D&E**)
574 Summary data (n = 21) of RA LTMR impulse frequency (**D**) and number (**E**) in the
575 ramp-up (circles) and ramp-down (squares) phases at the most sensitive angles. Data
576 represent mean ± SEM, *** $p < 0.001$.
577
578 **Figure 2. Angular tuning parameters and amplitude encoding of RA LTMRs**
579 **A**) Polar plot shows an example of angular responses of an RA LTMR. Solid and
580 dashed black lines indicate angular responses in the ramp-up and ramp-down phases,
581 respectively. Solid black arrow and dashed black arrow indicate vectors of the ramp-up
582 response and ramp-down response, respectively. Concentric circles and numbers
583 indicate impulse numbers. **B**) Bar graph shows numbers of RA LTMRs displaying
584 angular tuning in the caudal (caudal ± 45^o), ventral (ventral ± 45^o), rostral (rostral ± 45^o),
585 and dorsal (dorsal ± 45^o) directions. Black bars, ramp-up responses; grey bars, ramp-
586 down responses. Insert, tuning direction of each RA LTMR (n = 21). **C**) Histogram
587 shows the number of RA LTMRs with the angle sizes of high sensitivity. The angle size
588 of high-sensitivity was defined as the angle size at which responses were ≥ 80% of
589 maximal impulses. The bin is 30^o. Black bars, ramp-up responses; grey bars, ramp-
590 down responses. **D**) Histogram shows the number of RA LTMRs with different tuning
591 indexes. The bin of tuning index is 0.1. Black bars, ramp-up responses; grey bars,
592 ramp-down responses. **E**) Sample traces of RA LTMR impulses induced by a 50-μm
593 (top) and a 200-μm (bottom) ramp-and-hold deflection of a whisker hair in the most

sensitive direction. **F**) RA impulse numbers induced by whisker hair deflection at the most sensitive angle at the amplitudes of 10, 20, 50, 100, 200, 300, 400 and 500 μm (n = 5 for 10-200 μm, 4 for 300-400 μm, and 3 for 500 μm). Dotted line is the curve fitting the experimental data. Data represent Mean ± SEM.

Figure 3. Angular responses of SA1 LTMRs in whisker hair follicles

A) Sample trace (top panel) shows SA1 LTMR impulses in response to ramp-and-hold whisker hair deflection in 24 angular directions each at the amplitude of 200 μm. Whisker hair deflection at each angle is indicated under the sample trace. Bottom three traces are impulses at the expanded time scale from arrow-indicated angles in the top panel, one was the most sensitive angle (-30^{o} to the caudal direction) at which maximal numbers of impulses were evoked in both the dynamic and static phase (left panel), another was the angle at which impulses were evoked only in the ramp-up dynamic phase (middle panel), and the third was the angle at which impulses were evoked in both ramp-up and ramp-down dynamic phases (right panel). The sample traces were recorded from a left C3 whisker hair follicle. **B**) A different SA1 displaying impulses during the ramp-down dynamic phase (top panel) or impulses during and after ramp-down dynamic phase (bottom trace, post-ramp). The sample traces were recorded from a left C3 whisker hair follicle. **C**) Summary data (n = 19) of the sizes of the angles showing impulses in both dynamic and static phase (SA1), during and after ramp-down phase (post-ramp), only during dynamic phase (RA-like), and the sizes of the angles showing no response (null angle). **D**) Summary data (n = 19) of the angle sizes of RA-like subclasses with impulses only during ramp-up phase, impulses in both the ramp-up

and ramp-down phases, impulses only during the ramp-down phase. **E**) Instantaneous frequency of impulses at the most sensitive angle shown in A. **F**) Summary data (n = 19 recordings) of coefficient of variance of inter-event intervals of impulses at the most sensitive angles exemplified in A. **G**) Summary data (n = 19) of impulse frequency of SA1 LTMRs in the dynamic phase (234 ms) and static phase (4.75 s) at most sensitive angles exemplified in A. Data represent mean ± SEM, ***p < 0.001.

Figure 4. Angular tuning parameters and amplitude encoding of SA1 LTMRs

A) Polar plot shows an example of angular response of an SA1 LTMR. Arrow in the plot indicates the vector of the angular response. Concentric circles and numbers indicate impulse numbers. **B**) Bar graph shows the number of SA1 LTMRs displaying angular tuning to the caudal (caudal ± 45^{o}), ventral (ventral ± 45^{o}), rostral (rostral ± 45^{o}), and dorsal (dorsal ± 45^{o}) directions. Insert shows the tuning directions of each SA1 LTMR recorded (n = 19). **C**) Histogram shows distribution of SA1 LTMRs with the angle sizes of high sensitivity. The bin is 30^{o}. **D**) Histogram shows distribution of SA1 LTMRs with different tuning indexes. The bin of tuning index is 0.1. **E**) Sample traces show SA1 impulses induced by a 50-μm (top) and a 500-μm (bottom) ramp-and-hold deflection of a whisker hair in the most sensitive direction. **F**) SA1 impulse numbers induced by whisker deflection at the amplitudes of 10, 20, 50, 100, 200, 300, 400 and 500 μm (n = 4). Dotted line is the curve fitting the experimental data. Data represent mean ± SEM.

Figure 5. Angular responses of SA2 LTMRs in whisker hair follicles

A) Sample trace (top panel) shows SA2 LTMR impulses in response to ramp-and-hold whisker hair deflection in 24 angular directions each at the amplitude of 200 μm. Whisker hair deflection at each angle is indicated under the sample trace. Bottom three traces are impulses at the expanded time scale from arrow-indicated angles in the top panel, one was the angle at which impulses were evoked only in the ramp-up dynamic phase (left panel), another was the most sensitive angle at which maximal numbers of impulses were evoked in both the dynamic and static phase (middle panel), and the third was the angle at which impulses were evoked in both the ramp-up and ramp-down dynamic phases (right panel). The sample traces were recorded from a right D3 whisker hair follicle. **B**) A different SA2 displaying impulses during the ramp-down dynamic phase (top panel) or impulses during and after ramp-down dynamic phase (bottom trace, post-ramp). The sample traces were recorded from a right D3 whisker hair follicle. **C**) Summary data (n = 23) of the sizes of the angles showing impulses in both dynamic and static phase (SA2), during and after ramp-down phase (post-ramp), only during dynamic phase (RA-like), and the sizes of the angles showing no response (null angle). **D**) Summary data (n =23) of the angle sizes of RA-like subclasses with impulses only during ramp-up phase, impulses in both the ramp-up and ramp-down phases, impulses only in the ramp-down phase. **E**) Instantaneous frequency of impulses at the most sensitive angle shown in A. **F**) Summary data (n = 23) of coefficient of variance of inter-event intervals of impulses at the most sensitive angles exemplified in A. **G**) Summary data (n = 23) of impulse frequency of SA2 LTMRs in the dynamic phase (234 ms) and static phase (4.75 s) at most sensitive angles exemplified in A. Data represent mean ± SEM, *** $p < 0.001$.

Figure 6. Angular tuning parameters and amplitude encoding of SA2 LTMRs

A) Polar plot shows an example of angular response of an SA2 LTMR. Solid arrow indicates the vector of angular responses. Concentric circles and numbers indicate impulse numbers. **B**) Bar graph shows numbers of SA2 LTMRs that display angular tuning in the caudal (caudal ± 45^{o}), ventral (ventral ± 45^{o}), rostral (rostral ± 45^{o}), and dorsal (dorsal ± 45^{o}) directions. Insert is the tuning direction of each SA2 LTMR recorded (n = 23). **C**) Histogram shows distribution of SA2 LTMRs with the angle sizes of high sensitivity. The bin is 30^{o}. **D**) Histogram shows distribution of SA2 LTMRs with different tuning index. The bin of tuning index is 0.1. **E**) Sample traces of SA2 impulses induced by a 50-μm (top) and a 500-μm (bottom) ramp-and-hold deflection of a whisker hair in the most sensitive direction. **F**) SA2 impulse numbers induced by whisker hair deflection at the amplitudes of 10, 20, 50, 100, 200, 300, 400 and 500 μm (n = 6). Dotted line is the curve fitting the experimental data. Data represent mean ± SEM.

Figure 7. Comparison of angular tuning and amplitude encoding among RA, SA1, and SA2 LTMRs

A) Comparison of tuning index among SA1 (n = 19), SA2 (n = 23), and RA (n = 21). **B**) Comparison of the angle sizes of high sensitivity among SA1 (n = 19), SA2 (n = 23), and RA (n = 21). **C**) Comparison of angle sizes of null responses among SA1 (n = 19), SA2 (n = 23), and RA (n = 21). **D**) Comparison of impulse frequencies at the dynamic phase among SA1 (n = 19), SA2 (n = 23) and RA (n = 21). **E**) Comparison of the impulse frequencies at the static phase among SA1 (n = 19), SA2 (n = 23) and RA (n = 21). From A to E, impulses were elicited by whisker hair deflection at the amplitude of

200 μm in testing directions. Data represent mean ± SEM, * $p < 0.05$, ** $p < 0.01$, *** $p < 0.001$, ns, not significantly different.

Acknowledgement

We thank Dr. Ryan Vaden for comments on an earlier version of this manuscript. This study was supported by NIH grants NS109059, DE018661 and DE023090 to J.G.G.

Author contributions

J.G.G conceived research project. A.Y. and J.G.G designed and A.Y. performed experiments. A.Y., H.F. and J.G.G. analyzed data and participated data interpretation. J.G.G. and AY wrote the paper.

Declaration of Conflicting Interests

There are no financial or other relationships that may cause a conflict of interest.

References

Abraira, V.E. & Ginty, D.D. (2013) The sensory neurons of touch. *Neuron*, **79**, 618-639.

Adibi, M. (2019) Whisker-Mediated Touch System in Rodents: From Neuron to Behavior. *Front Syst Neurosci*, **13**, 40.

Bellavance, M.A., Demers, M. & Deschenes, M. (2010) Feedforward inhibition determines the angular tuning of vibrissal responses in the principal trigeminal nucleus. *J Neurosci*, **30**, 1057-1063.

Bush, N.E., Schroeder, C.L., Hobbs, J.A., Yang, A.E., Huet, L.A., Solla, S.A. & Hartmann, M.J. (2016) Decoupling kinematics and mechanics reveals coding properties of trigeminal ganglion neurons in the rat vibrissal system. *Elife*, **5**.

Ebara, S., Kumamoto, K., Matsuura, T., Mazurkiewicz, J.E. & Rice, F.L. (2002) Similarities and differences in the innervation of mystacial vibrissal follicle-sinus complexes in the rat and cat: a confocal microscopic study. *J Comp Neurol*, **449**, 103-119.

Furuta, T., Bush, N.E., Yang, A.E., Ebara, S., Miyazaki, N., Murata, K., Hirai, D., Shibata, K.I. & Hartmann, M.J.Z. (2020) The Cellular and Mechanical Basis for Response Characteristics of Identified Primary Afferents in the Rat Vibrissal System. *Curr Biol*, **30**, 815-826 e815.

Gottschaldt, K.M., Iggo, A. & Young, D.W. (1973) Functional characteristics of mechanoreceptors in sinus hair follicles of the cat. *J Physiol*, **235**, 287-315.

Halata, Z. & Munger, B.L. (1980) Sensory nerve endings in rhesus monkey sinus hairs. *J Comp Neurol*, **192**, 645-663.

Hemelt, M.E., Kwegyir-Afful, E.E., Bruno, R.M., Simons, D.J. & Keller, A. (2010) Consistency of angular tuning in the rat vibrissa system. *J Neurophysiol*, **104**, 3105-3112.

Ikeda, R., Cha, M., Ling, J., Jia, Z., Coyle, D. & Gu, J.G. (2014) Merkel cells transduce and encode tactile stimuli to drive Abeta-afferent impulses. *Cell*, **157**, 664-675.

Kwegyir-Afful, E.E., Marella, S. & Simons, D.J. (2008) Response properties of mouse trigeminal ganglion neurons. *Somatosens Mot Res*, **25**, 209-221.

Lee, S.H. & Simons, D.J. (2004) Angular tuning and velocity sensitivity in different neuron classes within layer 4 of rat barrel cortex. *J Neurophysiol*, **91**, 223-229.

Leiser, S.C. & Moxon, K.A. (2007) Responses of trigeminal ganglion neurons during natural whisking behaviors in the awake rat. *Neuron*, **53**, 117-133.

Lichtenstein, S.H., Carvell, G.E. & Simons, D.J. (1990) Responses of rat trigeminal ganglion neurons to movements of vibrissae in different directions. *Somatosens Mot Res*, **7**, 47-65.

Minnery, B.S., Bruno, R.M. & Simons, D.J. (2003) Response transformation and receptive-field synthesis in the lemniscal trigeminothalamic circuit. *J Neurophysiol*, **90**, 1556-1570.

Ranade, S.S., Woo, S.H., Dubin, A.E., Moshourab, R.A., Wetzel, C., Petrus, M., Mathur, J., Begay, V., Coste, B., Mainquist, J., Wilson, A.J., Francisco, A.G., Reddy, K., Qiu, Z., Wood, J.N., Lewin, G.R. & Patapoutian, A. (2014) Piezo2 is the major transducer of mechanical forces for touch sensation in mice. *Nature*, **516**, 121-125.

Rutlin, M., Ho, C.Y., Abraira, V.E., Cassidy, C., Bai, L., Woodbury, C.J. & Ginty, D.D. (2014) The cellular and molecular basis of direction selectivity of Adelta-LTMRs. *Cell*, **159**, 1640-1651.

Shoykhet, M., Doherty, D. & Simons, D.J. (2000) Coding of deflection velocity and amplitude by whisker primary afferent neurons: implications for higher level processing. *Somatosens Mot Res*, **17**, 171-180.

Sonekatsu, M. & Gu, J.G. (2019) Functional properties of mechanoreceptors in mouse whisker hair follicles determined by the pressure-clamped single-fiber recording technique. *Neurosci Lett*, **707**, 134321.

Sonekatsu, M., Yamada, H. & Gu, J.G. (2020) Pressure-clamped single-fiber recording technique: A new recording method for studying sensory receptors. *Mol Pain*, **16**, 1744806920927852.

Takahashi-Iwanaga, H. (2000) Three-dimensional microanatomy of longitudinal lanceolate endings in rat vibrissae. *J Comp Neurol*, **426**, 259-269.

Taylor, W.R. & Vaney, D.I. (2002) Diverse synaptic mechanisms generate direction selectivity in the rabbit retina. *J Neurosci*, **22**, 7712-7720.

Tonomura, S., Ebara, S., Bagdasarian, K., Uta, D., Ahissar, E., Meir, I., Lampl, I., Kuroda, D., Furuta, T., Furue, H. & Kumamoto, K. (2015) Structure-function correlations of rat trigeminal primary neurons: Emphasis on club-like endings, a vibrissal mechanoreceptor. *Proc Jpn Acad Ser B Phys Biol Sci*, **91**, 560-576.

779 Wellnitz, S.A., Lesniak, D.R., Gerling, G.J. & Lumpkin, E.A. (2010) The regularity of sustained firing reveals
780 two populations of slowly adapting touch receptors in mouse hairy skin. *J Neurophysiol*, **103**,
781 3378-3388.

782

783 Woo, S.H., Ranade, S., Weyer, A.D., Dubin, A.E., Baba, Y., Qiu, Z., Petrus, M., Miyamoto, T., Reddy, K.,
784 Lumpkin, E.A., Stucky, C.L. & Patapoutian, A. (2014) Piezo2 is required for Merkel-cell
785 mechanotransduction. *Nature*, **509**, 622-626.

786

787

Fig. 1

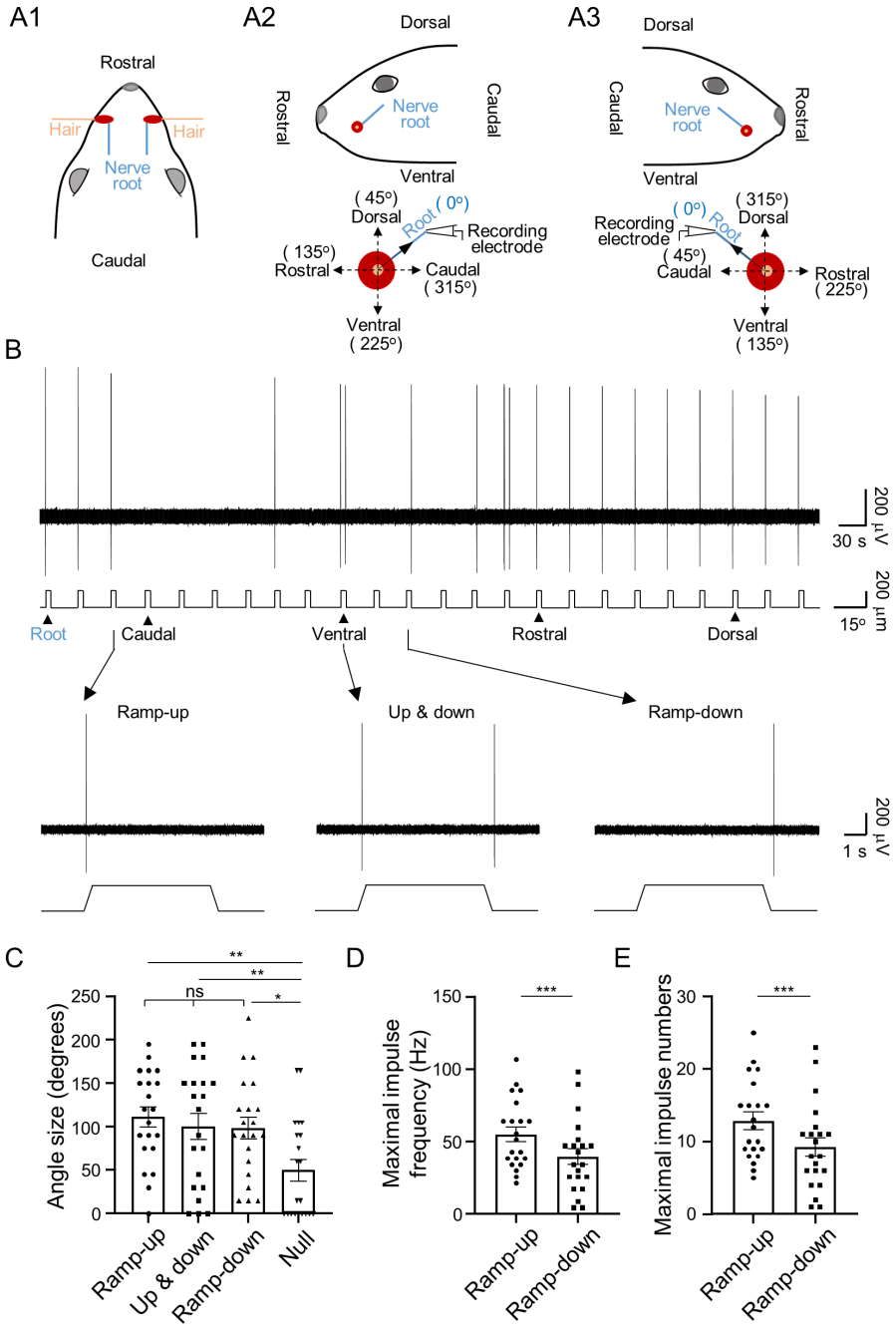

Fig. 2

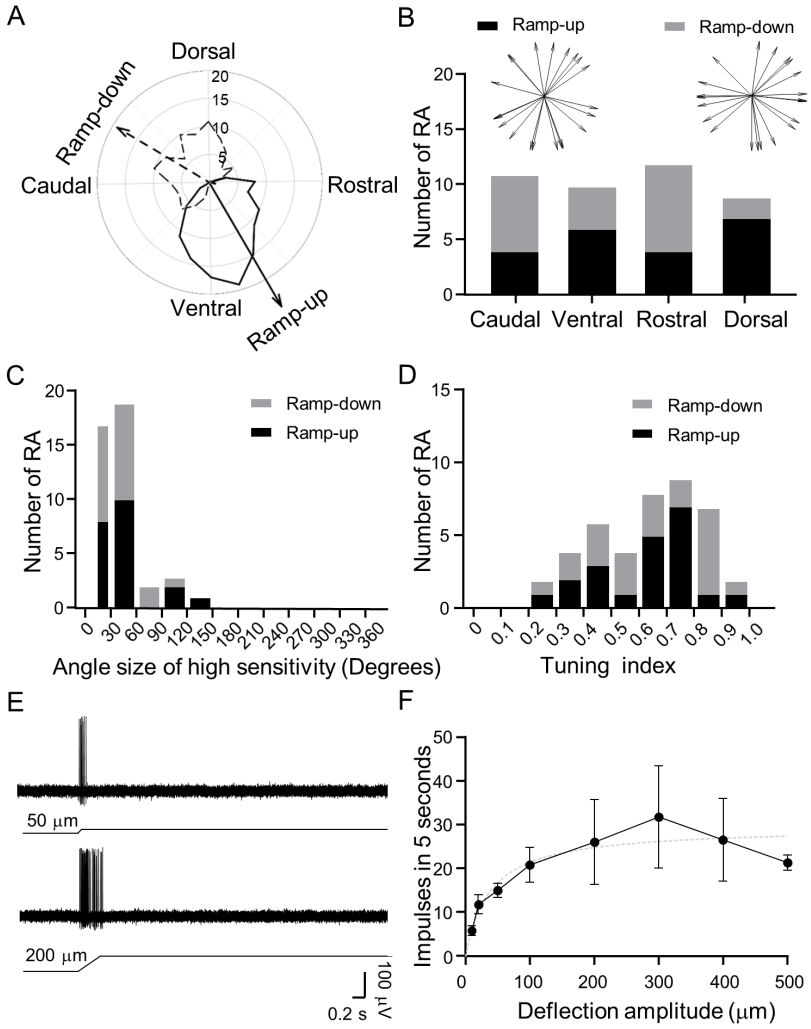

Fig. 3

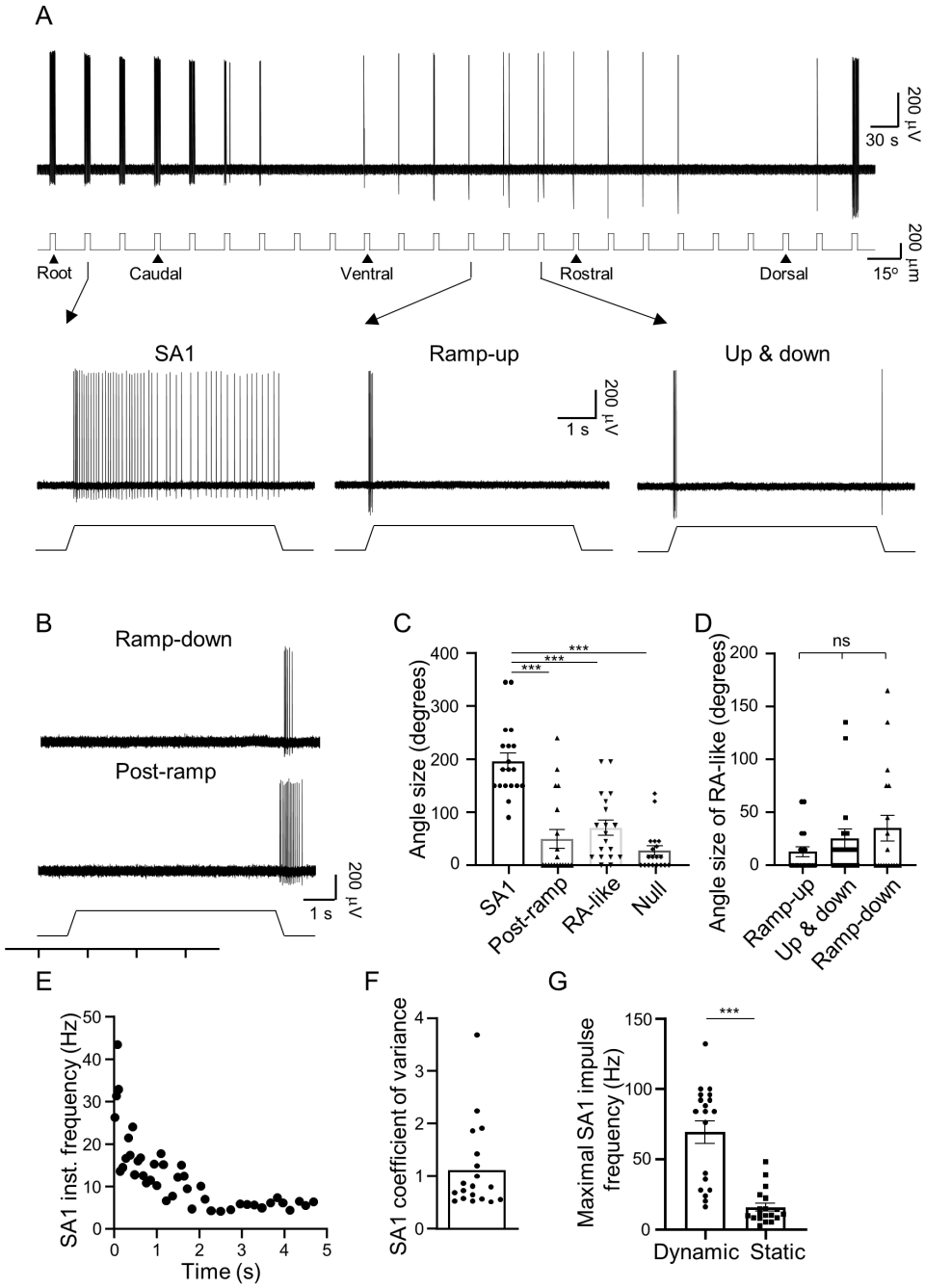

Fig. 4

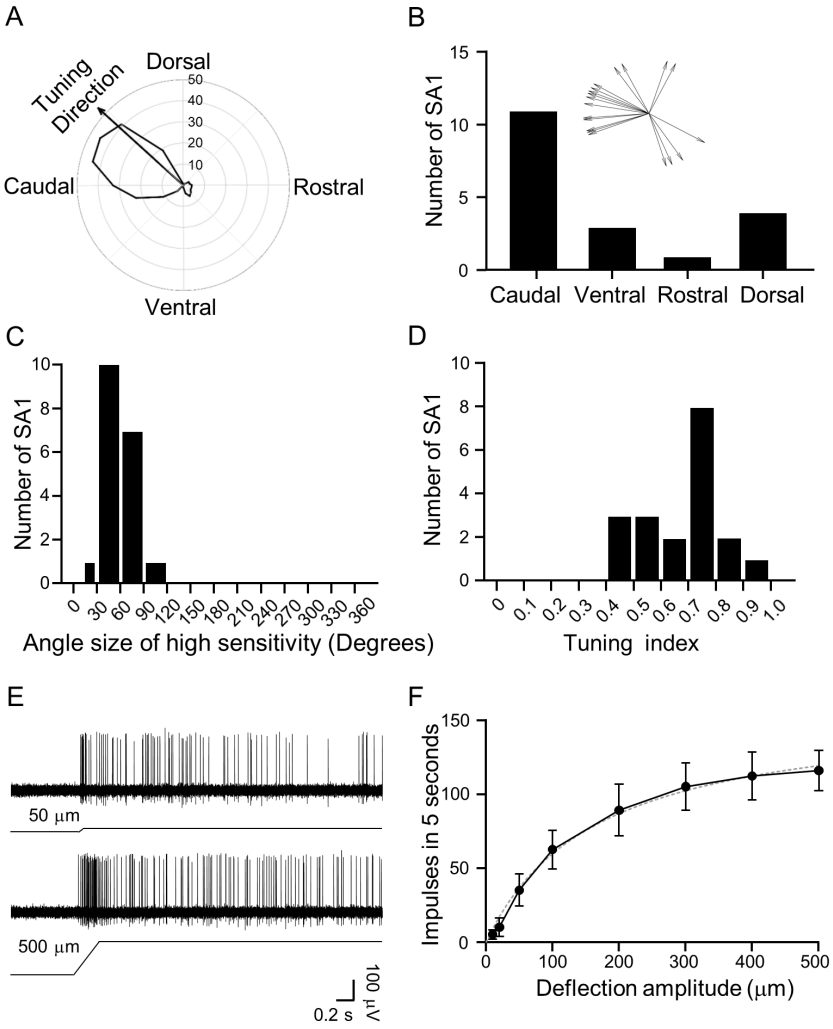

Fig. 5

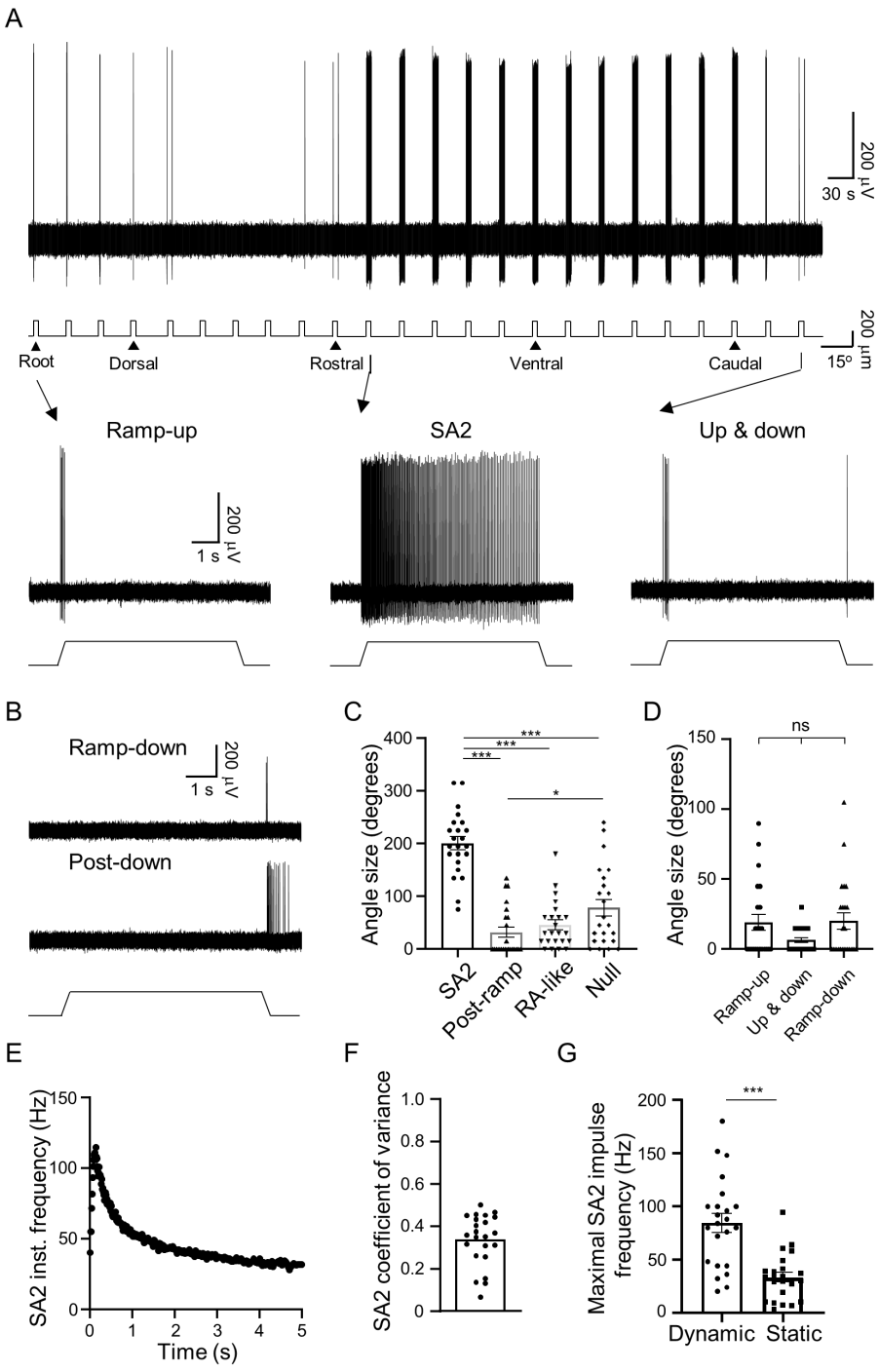

Fig. 6

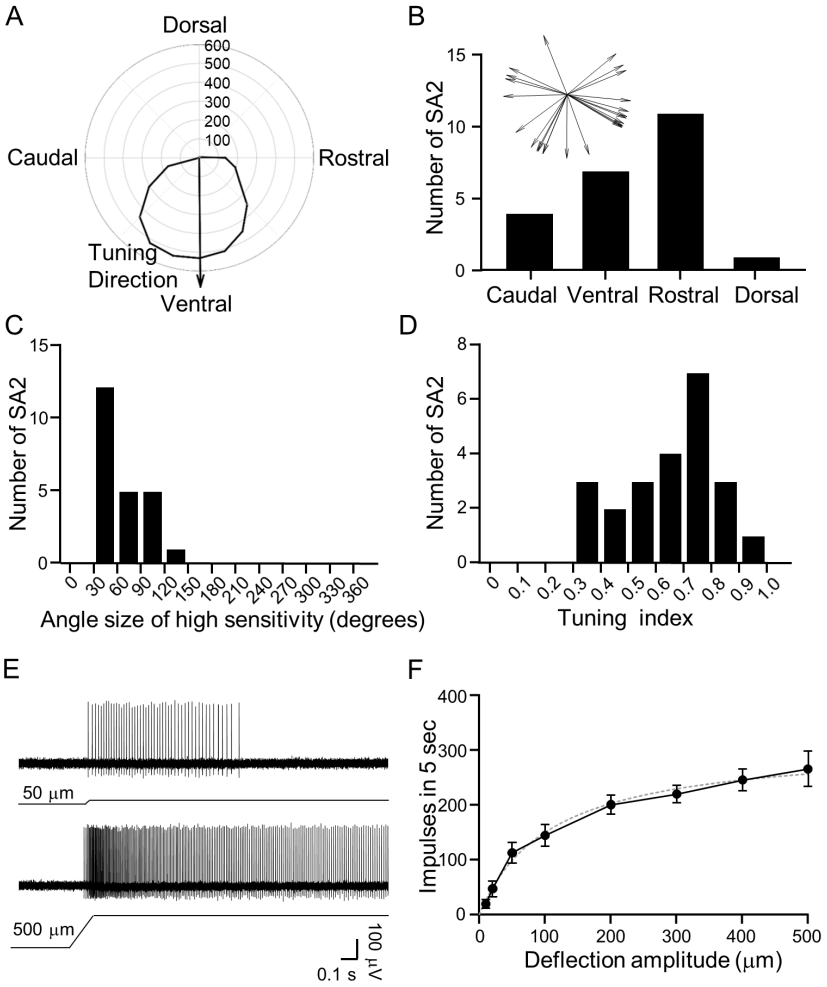

Fig. 7